

## EXOMARS IRAS (DOSE) radiation measurements

C. Federico<sup>1</sup>, A.M. Di Lellis<sup>2</sup>, S. Fonte<sup>3</sup>, C. Pauselli<sup>1</sup>, G. Reitz<sup>4</sup>, and R. Beaujean<sup>5</sup>

<sup>1</sup> Dipartimento di Scienze della Terra, Università degli Studi di Perugia, 06100 Perugia - Italy

<sup>2</sup> AMDL Srl, Viale Somalia 133, 00199 Roma - Italy

<sup>3</sup> INAF - Istituto di Astrofisica Spaziale e Fisica Cosmologica, via del Fosso del Cavaliere 100, 00133 Roma, Italy; e-mail: [sergio.fonte@iasf-roma.inaf.it](mailto:sergio.fonte@iasf-roma.inaf.it)

<sup>4</sup> German Aerospace Center Institut of Aerospace Medicine, 51147 Koeln - Germany

<sup>5</sup> Universitaet Kiel, IEAP/Extraterrestrik, Leibnizstr. 11-19, 24118 Kiel - Germany

**Abstract** The characterization and the study of the radiations on their interaction with organic matter is of great interest in view of the human exploration on Mars. The Ionizing Radiation Sensor (IRAS) selected in the frame of the ExoMars/Pasteur ESA mission is a lightweight particle spectrometer combining various techniques of radiation detection in space. It characterizes the first time the radiation environment on the Mars surface, and provide dose and dose equivalent rates as precursor information absolutely necessary to develop ways to mitigate the radiation risks for future human exploration on Mars. The Martian radiation levels are much higher than those found on Earth and they are relatively low for space. Measurements on the surface will show if they are similar or not to those seen in orbit (modified by the presence of “albedo” neutrons produced in the regolith and by the thin Martian atmosphere).

IRAS consists of a telescope based on segmented silicon detectors of about 40 mm diameter and 300  $\mu\text{m}$  thickness, a segmented organic scintillator, and of a thermoluminescence dosimeter. The telescope will continuously monitor temporal variation of the particle count rate, the dose rate, particle and LET (Linear Energy Transfer) spectra. Tissue equivalent BC430 scintillator material will be used to measure the neutron dose. Neutrons are selected by a criteria requiring no signal in the anti-coincidence. Last, the passive thermoluminescence dosimeter, based on LiF:Mg detectors, regardless the on board operation timing, will measure the total dose accumulated during the exposure period and due to  $\beta$  and  $\gamma$  radiation, with a responsivity very close to that of a human tissue.

**Key words.** Thermoluminescence – dosimeter – IRAS – TLD

### 1. Introduction

The Galactic Cosmic Rays (GCR atomic nuclei, stripped of their electrons) and the Solar

Particle Events (SPE protons and heavier ions) are of particular interest for astronauts voyages. Particularly for Mars’s ambient, that is notable unlike from Earth.

Mars lacks a global magnetic field, GCR particles arrive isotropically and are more en-

---

Send offprint requests to: S. Fonte

ergetic than those originating from Solar activity. SPE particles can occur randomly during the Solar cycle although they tend to occur near the peaks of Solar activity.

Sun radiates in all wavelengths, from radio (low energy) to X-rays and  $\gamma$ -rays (highest energy) through visible and infrared; the X-ray emission is highly variable. X-rays and  $\gamma$ -rays increase when Sun increases its activity (1-2 orders of magnitude).

There are two kinds of SPE: the Solar Wind and the Solar Energetic Particle (SEP). The first ones are charged particles continuously expelled from the Sun: electrons, protons and alpha particles (Helium nuclei) with low speed and low energy. They are carried along solar magnetic field and modulated by solar cycle (max at solar max), with an energy of about 1 keV/nucleon.

While the second are charged particles expelled from the Sun at high speed and high energy, related to extreme events on solar surface. They are sporadic and unpredictable, with an anisotropic distribution (following magnetic lines). They tend not to happen at solar min; their energy is about of 10-100 MeV/nucleon and it can be greater.

The GCR are charged particles from supernova explosions at very high speed accelerated by galactic magnetic field; they are composed of protons (85%),  $\alpha$  (12.5%), heavier atoms (1%) and electrons (1.5%) with an isotropic distribution. Their intensity are modulated by solar cycle (~11 years); Min at solar max. Their energy is about of 50-500MeV/nucleon (which means 10sof GeV for heavy ions).

The interplanetary space is unshielded, full of GCR and solar particles, while near the Earth, most of solar particles are shielded by the Earth's magnetic field, adding effects to the trapped particles (mostly protons and electrons) in Van Allen belts, from 4000 km to 10000 km in altitude. On the surface, the particles are shielded by atmosphere. On Earth, we have an average of 2.4 mSv/year, due to space (17%) and natural radiactivity (83%).

In the Mars Odyssey mission (that is part of NASA's Mars Exploration Program), the calculations of MARIE, the Martian Radiation Environment Experiment for studying the ra-

diation environment, estimate about 1 Sv/year on Mars surface.

Another radiation comes from Mart's rock. Martian crust has a bulk composition equivalent to large-ion lithophile (LIL) and heat producing element (K, Th, U) enriched basalt, with a potassium content of about 0.5% and Martian Dose Rate = 240 nGy/h (max estimation), see McLennan (2001).

All these radiations interact primary with the spacecraft structure and after with the astronauts tissues, producing secondary radiations and particles.

The absorption of all this energy by cellular molecules causes several effects (cell death, molecular breakage and cell genetic mutation) leading to an increase in the cancer developing probability.

Every tissue show a different tolerance to dose. Usually, three organ types are considered: the skin (outside part, unshielded), the eyes (specially sensitive organs) and the Blood Forming Organs (BFO, bone marrow): deeper organs, highly self-shielded.

There is in the ExoMars/Pasteur mission an instrumentation to estimate the risk of interaction between the radiation and the human's tissues. It combines a principal sensor: Ionizing Radiation Sensor (IRAS) and an optional Thermo Luminescence Detector with the annexed reader: TLD Reader (formerly named DOSE). IRAS, whose leadership is German, is the instrument actually selected for Exomars/Pasteur mission.

## 2. Ionizing Radiation Sensor (IRAS)

The Ionizing Radiation Sensor (IRAS) selected in the frame of the ExoMars/Pasteur ESA mission is a lightweight particle spectrometer combining various techniques of radiation detection in space. Its design from heritage components makes it a powerful experiment to deliver at minimum risk outstanding scientific data.

It characterizes for the first time the environment radiation on the Mars's surface, and provides dose and dose equivalent rates as precursor information absolutely necessary to de-

velop ways to mitigate the radiation risks for future human exploration on Mars.

The silicon detector telescope sensor of the instrument uses segmented silicon detectors and it will continuously monitor temporal variation of the particle count rate, the dose rate, particle and LET spectra. During operation two types of measurements will be performed:

- a) single detector mode for dose measurements in the individual detectors;
- b) coincidence mode for the measurement of particle and Linear Energy Transfer (LET) spectra in the range 2 to 2000 MeV/cm.

Both measurements are an integration over software defined time periods resulting in a reasonable data reduction. LET spectra will be deduced from the energy deposit of coincident events in the silicon detectors. Since the incidence angle of the particles is not measured, the energy deposit is converted into LET in silicon, as energy deposit/ $t$ , where  $t$  is the mean path length in the detector.

The detector telescope of the IRAS will work in one mode only. In this mode data for count and dose rates will be integrated over pre-selected time intervals, a typical interval may be 10 minutes. These time intervals are software dependent and can be adjusted within reasonable counting statistics. Data provided are time resolved count and dose rates (separate measurement of charged and neutral components) and the measurement of the LET spectrum. LET values in water from about 2 MeV/cm (minimum ionisation for singly charged particles) to 2000 MeV/cm are covered.

All data will be stored temporally in an internal histogram memory. Data need to be downloaded and transferred to ground. The maximum data rate is 1 Mb/day.

The coincidence requirement between the two detector signals of the telescope selects particles with restricted pathlength in the planar detectors (the angle of the acceptance cone is about 120°). The LET(Si) values are deduced from the measured energy, deposited in the individual silicon detectors in coincidence mode, using a mean pathlength of 364  $\mu\text{m}$  at a density of 2.33 g/cm<sup>3</sup>. This procedure under-

estimates the LET value of short range particles stopping inside the detector. In order to account for the difference in stopping power of Si and water, the LET(Si)-value is multiplied by a factor of 1.23 to get the LET(H<sub>2</sub>O)-value. This mean conversion factor neglects the dependence on the particles energy, the uncertainty is estimated to be 3%.

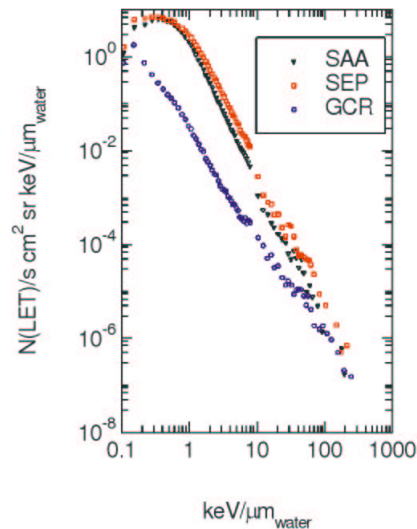


**Figure 1.** LET spectra for three components: a GCR particles, solar energetic particles during the April 15, 2001 event (SEP) and radiation belt particles (SAA).

In Figure 1 shows the measured LET spectra converted to water for the three radiation fields components which could be separated. The shape and gradient of the LET spectrum defines the mean radiation quality factor  $Q$  calculated with  $Q(\text{LET})$ -values. It is obvious that the GCR spectrum has the lowest gradient and thus the highest  $Q$ -value.

The IRAS consists of three segmented planar silicon PIN-detectors (300  $\mu\text{m}$  thickness, outer diameter 42 mm) and a segmented solid organic scintillator (BC430), with an outer diameter of 50 mm and a thickness of 15 mm. BC430 is an orange-emitting scintillator that has a nominal wavelength peak emission near 580 nm. BC430 is conventionally used in radi-

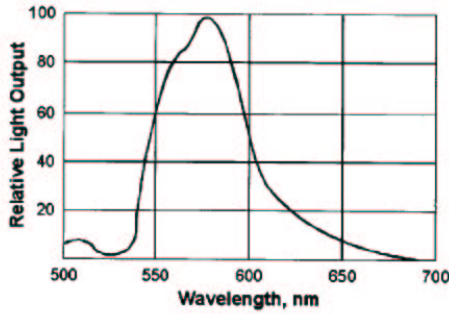


**Figure 2.** The BC430’s emission spectrum in the red region, credit Saint-Gobain Crystals

ation detector applications because of its high light output and because of the high quantum efficiency of PMTS in this part of the spectrum.

Two additional silicon sensors serve for measurements of particle count rates and dose rates in the two remaining directions. Tissue equivalent BC430 scintillator material will be used to measure the neutron dose. The scintillator is surrounded by an anticoincidence detector, build up from the telescope and a scintillator ring. Neutrons are selected by a criteria requiring no signal in the anti-coincidence detectors. The energy spectrum of recoil protons from neutron interactions will be measured in the range 1 to 30 MeV.

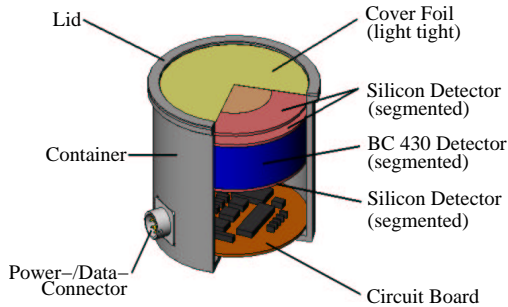


**Figure 3.** The IRAS instrument plan consists of three segmented planar silicon PIN-detectors and a segmented solid organic scintillator

The outer segment of the scintillator and part of the silicon detectors act as anticoincidence shield for the inner part of the scintillator

(26 mm diameter, 15 mm height, see Figure 3). The detector telescope sensor is built up by the inner segments (26 mm diameter) of two planar silicon detectors. The third Si-detector is in optical contact with the scintillator and provides for the light detection.

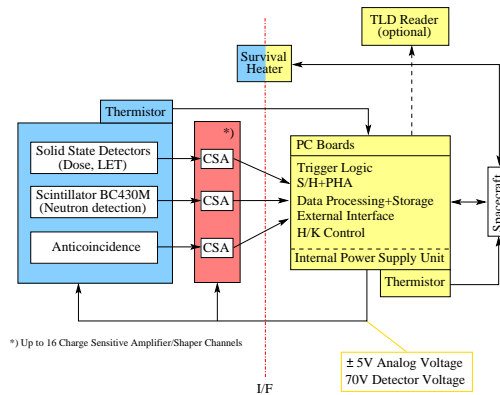


**Figure 4.** IRAS Electrical design

Two additional PIN diodes are added in the electronic part beneath the detector head to provide measurements in *x* and *y* direction. The size of the detector system is 58 mm in diameter and 55 mm in height, the mass is about 500 g with a power consumption of 600 mW. The operation of the system is managed by a microcontroller which controls the operation mode by switching the power and data lines to the individual sensors via multiplexer on the main board, data sampling, internal intermediate storage and data transfer to the external main storage. The instrument uses a RS 422 interface. Similar designs are used for MATROSHKA sensors and for the detector telescope DOSTEL on EuTEF.

In Figure 4 is represented the IRAS electrical design, with an optional insertion of a TLD Reader.

The IRAS instrument is capable to characterize the radiation field concerning particle fluences, dose rates and energy transfer spectra for ionising particles. In addition, it allows to determine the dose contribution of secondary neutrons from GCR-interactions with the atmosphere and the soil.

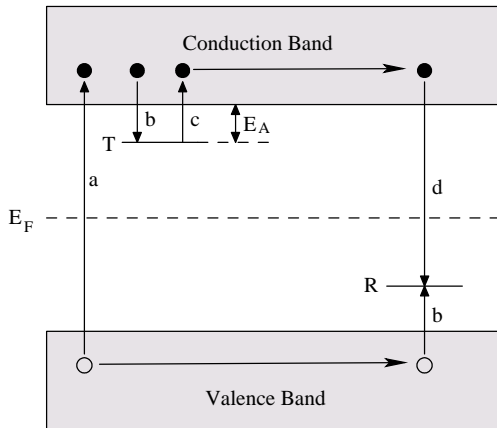


**Figure 5.** Energy band model showing the electronic transitions in TL material according to a simple two-level model: (a) generation of electrons and holes; (b) electron and hole trapping; (c) electron release due to thermal stimulation; (d) recombination. Solid circles are electrons, open circles are holes. Level T is an electron trap, level R is a recombination centre,  $E_F$  is Fermi level. See Bos (2001)

The measurement will be carried out on Mars, during cruise and in orbit. The IRAS instrument just need to be powered for ten minutes each hour, during cruise permanent operation would be preferred. After switch/on measurements are started automatically. Data transfer to the DPHU of the rover/GEP shall be done at the end of the measuring period. The measuring intervals provide enough information to draw a complete time dependence profile of the radiation environment.

### 3. The TLD Reader

The TLD Reader is designed to keep track of the radiation exposure field when the astronauts will pass through during both the *surface* stay and during the *transit* period to and from the red planet.

The TLD Reader instrument is a passive dosimeter working without any powering or support after the annealing. It will not suffer for any gap during measurements and will collect energy even in presence of huge SPE.

The TLD Reader will only measure the integrated energy over some period of time (dif-

ferent phases of the cruise and of the surface exploration) and will be able to measure  $\beta$  and  $\gamma$  radiation dose. The TLD Reader has a responsivity very close to that of a living organism, Bos (2001).

The TLD Reader is based on doped thermoluminescence lithium-fluoride passive detectors (pills of LiF:Mg,Cu,P). An explanation of the observed ThermoLuminescence (TL) properties can be obtained from the energy band theory of solids (with one trap-one centre model), as noted by Bos (2001).

In Figure 5, it is represented a pattern of the one trap-one centre model. As result of interaction with the radiation, some electrons are trapped in the T state inside the gap energy; it is a non-equilibrium state.

The relaxation rate for the T state is determined by Arrhenius's probability, see Bos (2001). More high is the temperature, greater is the transition probability from T state to conduction band, and greater is the recombination in the R state.

The recombination produces a  $\gamma$  ray in the visible range, so called thermoluminescence signal. A thermoluminescence photons' count estimates the absorbed dose by semiconductor dosimeter. Usually to read the TL signal, the TL material is stimulated with a thermal pattern, for example, a linear stimulus; this stimulus produces a response so called glow curve. This curve is composed of peaks.

These peaks represent a dopant (or a defect) of the semiconductor dosimeter. There is an evident peak, so called 4-peak, at about 240 °C for the LiF:Mg,Cu,P. The integral of glow curve gives the number of trapped electrons in the T state, then the dosimeter's absorbed dose.

The environmental monitoring of radiation doses using with TL detectors is extremely valuable companion to environmental monitoring using systems equipped with active, on-line dosimeters, see Olko et al. (2004).

TLD are used for long term (about 3-12 months) environmental dosimetry, around nuclear installations. The so called high sensitive on LiF:Mg,Cu,P is about two orders of magnitude more sensitive than conventional LiF(TLD-100), which enables short term (2

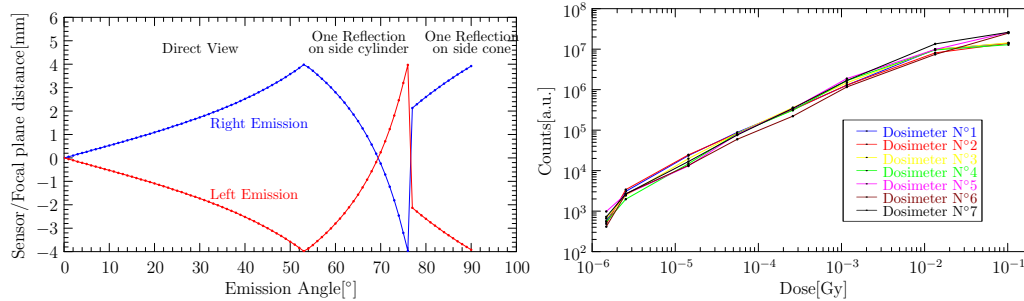


**Figure 6.** The photon's impact dynamics on the conical collector, from central point of dosimetral. On the right the tests on detectable dose ranges

weeks, against 3 months exposure) radiometry surveys of the environment. This high sensitivity also allows short-term (hourly or daily) monitoring of local changes of radiation doses after substantial contamination of the environment, see Olko et al. (2004).

The capacity of these detectors to integrate the received energy from their last reset, would be used to measure the possible collected doses during different phases of the mission: cruise phases, permanence on Mars.

The measure process is based on the photons counting of luminescence radiation emitted during the detectors heating cycle.

TLD can't measure the heavy component, but recent works of Cucinotta et al. (2002) and those of Saganti et al. (2002) have shown that the heavy component on the total accumulated dose results to be a negligible part in the Martian environment.

The detector is placed in a silver oven, and kept in place by means of a mechanical fixture (no adhesives). The mini oven is heated by means of a thermofoil<sup>TM</sup> heater with mica insulation, able to withstand the 240 °C temperature. The heater is clamped by means of a steel plate.

The collection of light is enhanced by a conical collector. The collector's geometry optimises the signal acquisition, providing an effective shielding for radiative heating towards the photomultiplier tube.

In Figure 6, it is represented the impact on the conical collector versus the photons' angles emission from central point. It is corresponded to each angle a particular impact: there is a di-

rect collection of photons on the counter (direct view), or a collection after one reflection on side cylinder, or a collection after one reflection on the side cone.

To optimise the collector's geometry, the optical ray impact on the conical collector only one time.

A filter is placed in front of the tube, limiting the useful waveband to the range of 300÷500 nm, reducing the infrared radiation entering the tube itself.

In Figure 6, it is represented the response of system detector to different doses absorbed from a <sup>109</sup>Cd source.

The linear response of the LiF:Mg,Cu,P is from 1 µGy to 10 Gy; the down to high doses is caused from a slow response of electrical circuit used to read the TL signal from dosimeter pill (a laboratory multifunction reader). While the low doses non linear response probable is due to a dosimeter's sensibility. Nevertheless, the response is good and maybe when the reader is optimized, these diffects will disappear.

In Table 3 is reported the weight (in grams) of the all system (IRAS+TLD Reader). It is important to note that the passive sensor even thought is not able to provide an instantaneous measurement of the dose rate, it is conversely able to return a total dose measurement very close to that a human tissue could accumulate during any phase of the mission with no power request to the system, being completely passive operated.

The advantages of passive detectors for environmental monitoring are that they are:

**Table 1.** Mass breakdown of the all radiation detector

Item	Sub-Item	Weight [g]
Telescope	Housing & conn.	120
IRAS	<i>Detector head</i>	
	-Scintillator	60
	-Silicon detectors	40
	-Frame	120
	Electronics	160
Subtotal		500
TLD	Collimator	12
Reader	Structure	91
	Detector & Holder	15
	Phototube	15
	HV Block	35
	Electronics	35
	Harness & conn.	30
Subtotal		228
Total		728

small, cheap, don't require in situ electronic

power supply and can be used in a large dose range.

They provide measurements of the dose integrated during the time interval (days months) which means that only an average dose rate value for this period can be estimated.

## References

- Bos, A. J. J. 2001, Nucl. Instr. and Meth. in Phys. Res. B, 184, 3
- Chen, T.C. and Stoebe, T.G. 1998, Rad. Meas., 29, 39
- Cucinotta, F. A. and Saganti, P. B. and Wilson, J. W. and Simonsen C. 2002, J. Radiat. Res., 43, 35
- Olko, P. and Budzanowski, M. and Bilskil, et al. 2004, Nucl. Tech. and Rad. Prot, 19, 20
- Saganti, P. B. and Cucinotta, F. A. and Wilson, J. W. 2002, J. Radiat. Res., 43, 119
- Garlick, G. F. J. and Gibson, A. F. 1948, Proc. Phys. Soc., 60, 574
- McLennan, S.M. 2001, Geophys. Res. Lett., 28, 4019